Eng. Sci., 2022, **20**, 364–376

Engineered Science

DOI: https://dx.doi.org/10.30919/es8d780

Investigation of Photoelectric Properties, Substrate Effects and Structural Identification of Layered Rutile Titanium Oxide with χ3 of Borophene using Density Functional Theory

Ayotunde Idris Ibitoye,[#] Oriyomi Opetubo,[#] Sunday Temitope Oyinbo,[#,*] Tien-Chien Jen,[#,*] David Sibanda[#] and Ewuola Oluwatoyin[#]

Abstract

Titanium Dioxide is an attractive material used for photovoltaic and photocatalytic purposes. Borophene is a newly produced metallic sheet that resembles graphene in many ways and is expected to complement graphene as a high density of states, optically transparent two-dimensional (2D) conductor. This study looked at the photoelectric potential of a borophene/TiO bilayer by analyzing the interface's atomic-level interactions and electronic properties using density functional theory (DFT). Rutile TiO_2 (001) was combined with χ3 of borophene in a nanocomposite with high interfacial coupling to study the photoelectric characteristics, substrate effects, and structural identification of Rutile TiO_2. An adequate DFT approach for bulk TiO_2 and Borophene, verifying the Perdew-Burke-Ernzerhof method's accuracy, was first established. Low interplanar distances and high adhesion energies were found in the optimized structures, indicating good interfacial interaction. With a band gap of ~0.369 eV, the electronic band structure and density of states (DOS) revealed its Potential superconducting nature. The absorption coefficient, reflectivity, refractive index, dielectric function, optical conductivity, and electron energy loss function are among the other optical properties that have been identified. It is possible to modify the work function for both of the materials in the study, enabling their prospective usage as Superconductors and gas sensor devices.

Keywords: Borophene; Titanium Dioxide; Semiconductor; Work function; Charge Density.
Received: 30 August 2022; Revised: 26 September 2022; Accepted: 06 October 2022.
Article type: Research article.

1. Introduction

Until recently, theoretical research predicted the development of new varieties of two-dimensional (2D) boron sheet structures, including G/α /β/γ type and less stable hexagonal and triangle sheets.[1] A recently created metallic sheet called borophene is predicted to work in conjunction with graphene as a 2D conductor with a high density of states and optical transparency. 2D materials have many applications in electronics, energy storage and use because of their unique physical and chemical properties (such as linear band structure around the Fermi level, stiffness, thermal and electrical conductivity).[2,3] When understanding material characteristics, distinguishing a 2D material from other surface features is critical since the system's key attributes can be substantially influenced by its location relative to the supporting substrate.[4] The interface structure affects strain, doping, and symmetry of the 2D overlayer, as well as a Van der Waals Force (vdW) bonded 2D material. It is possible to conclude that the study will play an essential role in the development of current technologies based on the projected qualities. Recently, many 2D materials have been theoretically predicted and synthesized experimentally.[3,4]

After carbon, boron is the second element to possess a variety of low-dimensional anisotropic structures. Because of this growing interest, new solids, quasiplanar clusters, nanosheets, nanotubes, nanowires, nanoropes, nanospheres, nanobelts, nanoribbons, and quasicrystals made of pure boron have been developed.[5] Boron's bulk 2D layered structures are common in nature, unlike graphene and some other 2D materials, due to the atomic arrangement of boron in the crystal lattice, which acts as a driving force to produce more curved and wavy structures. This makes mechanical exfoliation difficult in experimental synthesis. Therefore, only thermal evaporative deposition, chemical vapor deposition, or molecular beam epithelium can be used in the experimental synthesis of 2D boron monolayers.[5]

Due to the high concentration of Fermi-order carriers

Department of Mechanical Engineering Science, University of Johannesburg, 2006, South Africa.
[#]*These authors contributed to this work equally.*
**E-mail:* soyinbo@uj.ac.za (S. T. Oyinbo); tjen@uj.ac.za (T-C. Jen)

absent in graphene with zero density charge carriers at the Dirac cone, atomically thin borophene is an ideal platform for studying the distribution and response of electron gases confined to an ultrathin layer with external disturbances.[4] The stability of borophene is enhanced by physically or chemically bound species. Long wavelength imaginary modes still exist in single triangular plates and other polymorphs such as β_{12} sheets, according to first-principles phononic computations.[2] Recent theoretical work has suggested that using a substrate or chemical function to modulate the adsorption and energy of borophene might be a viable option.[6,7]

To synthesize 2D boron sheet, the substrate needs to be carefully selected. Wu *et al.*[1,8] in 2016 produced Ag(111) stabilized 2D Boron sheets. It has been reported that the pore density in the structure of β_{12} and $\chi 3$ composites, as well as bulked borophene, exceeds 1/8. The epitaxial growth of graphene on Cu(111) suggests that the desired substrate for 2D borophene must have low boron solubility while acting as a planar template.[4] Many metals, including those commonly used to grow carbon nanotubes, are known to produce borides (Fe, Co, Ni).[6] Cu, Ag and Au are members of Group 11 and do not produce borides; therefore, they were chosen as substrates to simulate boron deposition.[6] The octet rule requires the boron atom to be paired with five extra electrons because it contains three valence electrons. According to band theory, each boron atom is bound to six neighbors in borophene, preferring the metallic phase. The localization of borophene's moving electrons and the opening of its band gap is an intriguing topic for electronic applications.[4]

Various studies have shown that borophene possesses inherent metallicity, optical transparency, high flexibility, tunable properties, and high-temperature superconductivity due to its rich structural properties. Farideh *et al.*[1] investigated the decoration of $\chi 3$ borophene with Fluorine atoms for the anodic performance of Lithium-ion batteries by means of density functional theory. Also, in the computational examination, the report revealed the need to address the many configurations that come from decorating a structure with sufficient thermodynamic and kinetic stability. Khawla *et al.*[9] experimentally showed that the optoelectronic characteristics and stability of the $MAPbI_{3(1\ x)}B_{3x}/ZnO$ heterojunction are respectively enhanced by Br doping, using a spin coating technique. Zihan *et al.*[10] studied the adsorption of the halogen atom on $\chi 3$ borophene, followed by the adsorption of one Li atom on the resulting sheet, and found that if the diffusion barrier for Li is enhanced, it requires more processing, especially for $\chi 3$ borophene.

Considering the unique properties and wide application of borophene, the attempts to modulate the hydrogen storage effect, Li storage effect, adsorption efficiency, electronic properties, magnetic properties and properties of borophene optics is still in their infancy; Further research focusing on tuning the properties of borophene is still needed. Based on our knowledge, there are no relevant studies on altering the photoelectric properties of borophene, especially in the field of semiconductor optoelectronics.

In this study, we focus on the effect of substrate surface absorption (interfacial contact) on the photoelectric properties of $\chi 3$ borophene by using density functional pseudopotential plane-wave methods. We investigated the stability of the $\chi 3$ borophene sheet when interfaced with Rutile TiO_2 (001) phase and its superconductivity structure. The above-mentioned is the novelty of this research. The electronic structure, substrate effects, structural identification, lattice dynamics, and optical properties of the $\chi 3$ borophene sheet supported by Rutile TiO_2 (001) were analyzed before and after the substrate interface. The study results provide a theoretical basis for the application of borophene in the area of semiconductor optoelectronics.

2. Computational method and model

For the electronic structure calculations, the plane-wave basis projector augmented wave method[11] was employed in the Spin-polarized density functional theory (DFT) approach framework. This was done within the generalized gradient approximation in the Perdew Burke–Ernzerhof (PBE) form[12] as implemented in the VASP code.[13,14] A plane-wave energy cutoff of 520 eV and an energy convergence criterion of 10^{-8} eV was used. A 20 × 20 × 1 k-point sampling mesh was used for the unit cell, and the equivalent density mesh was used for the supercells together with a 0.05 eV smearing width of the Methfessel–Paxton scheme.[15] A 15Å vacuum space along the out-of-plane direction is created to avoid false contact between periodical images. All structures are relaxed until the forces drop below 0.01 eV $Å^{-1}$. For the work function calculations, the Heyd–Scuseria–Ernzerhof hybrid function (HSE06)[16] is used to explain the self-interaction and screen the carrier more appropriately.

The computational model of the $\chi 3$ borophene sheet contains 28 boron atoms, and the lattice constants are a = 9.307 Å, b = 9.307 Å, respectively. Due to phonon instability, this phase is dynamically unstable in the autonomous state.[17,18] In addition, a model containing 7 boron atoms was made to form a heterogeneous structure with rutile TiO_2 (001) containing 12 Titanium atoms (Ti) and 24 atoms of Oxygen (O). The heterostructure model is shown in Fig. 1(a) before relaxation and interfacing, and Fig. 1(b) shows the interfaced structure created after binding and adsorption.

The adsorption energy of $\chi 3$ borophene sheet on Rutile TiO_2 (001) substrate was calculated as follows[1,18,19],

$$E_{ads} = \frac{E_T - E_{T_iO} - n_B E_{\chi^3}}{n} \quad (1)$$

where E_T is the total energy of the heterogeneous system, n_B is the number of B atoms in the system, n is the total number of atoms in the system, E_{χ^3} is the energy of a single isolated B atom in the system, and E_{T_iO} is the total energy of the substrate without adatoms. The application of first-principles calculations in condensed matter physics and materials science has grown significantly as phonon calculations have become routine over the past decade.

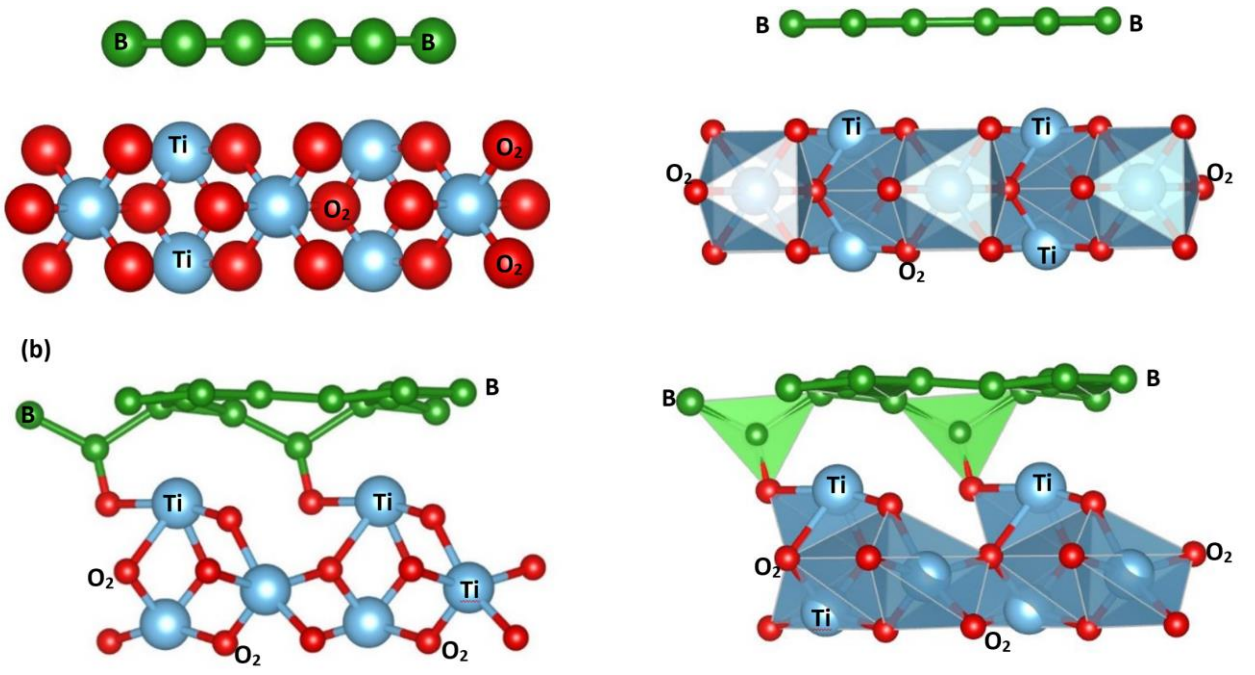

Fig. 1 (a) χ3 borophene sheet before relaxation and interfacing with Rutile TiO_2 (001) substrate (b) χ3 borophene/ Rutile TiO_2 (001) substrate Interfaced structure created after binding and adsorption.

The binding energy (E_B) of χ3 borophene sheet on Rutile TiO_2 (001) substrate was used to determine their energetic stability.[20,21]

$$E_B = E_{X^3} + E_{Ti_O} - E_{Ti_O + X^3} \quad (2)$$

Where $E_{TiO+\chi 3}$ is the total energy of χ3 borophene sheet absorbed on Rutile TiO_2 (001) substrate, $E_{\chi 3}$and E_{TiO} are the total energies of the isolated χ3 borophene sheet before absorption and the Rutile TiO_2 (001) substrate before absorbing. An exothermic process correlates to a positive E_B value.

3. Results and discussion

3.1 Electronic and structural properties

The Optimal lattice parameters of χ3 borophene sheet on TiO_2 (001) substrate are a = 4.45 Å , b = 4.32 Å , c = 9.56 Å with corresponding angles of $\alpha = 86.07°$, $\beta = 88.70°$, and $\gamma = 83.51°$ gives a reasonable agreement with the value reported by Fazilaty *et al.*[18] χ3 borophene monolayers phase has been reported in the literature to be dynamically unstable at rest due to its phono instability. This unstable phase is expected to be trapped in a metastable state and stabilized by charge transfer to the underlying TiO_2 (001) substrate; thus, the dynamic instability will gradually decrease. Fig. 2(a) displayed the relaxed structure of the χ3 borophene sheet on TiO_2 (001) that remains planar on the substrate. The vertical distance between the χ3 borophene sheet and TiO_2 (001) surface is 1.38 Å, as shown in Fig. 2(b). The adsorption energy -1.67 eV or -0.24 eV/Atom of χ3 borophene sheet on TiO_2 (001) was calculated using Eq. (1) indicated above. The negative adsorption energy values show favourably.

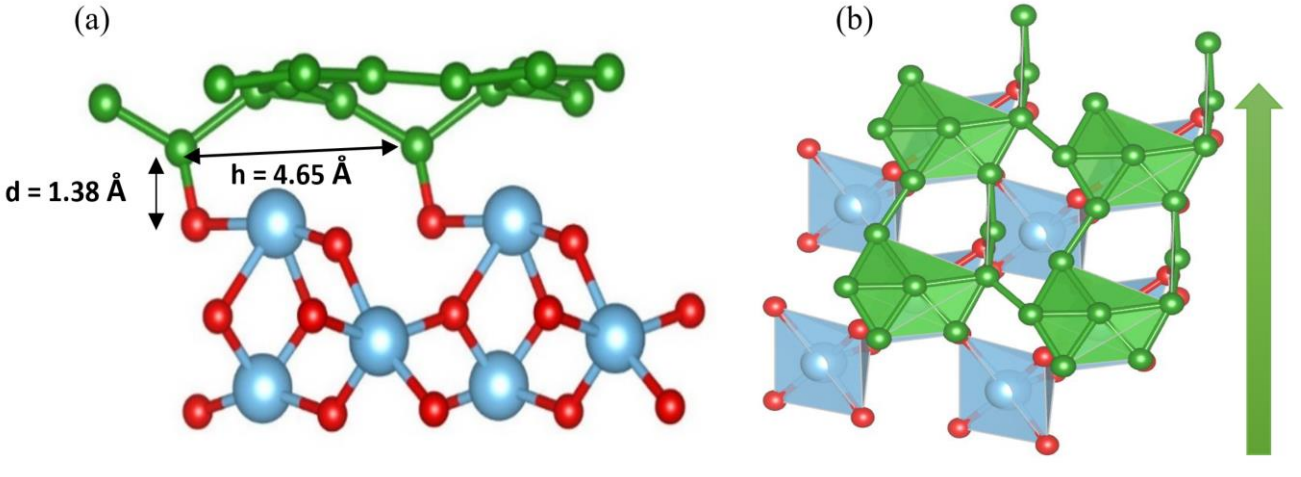

Fig. 2 (a) the Interfacial coupling of χ3 borophene to TiO_2 (001) substrate. (b) χ3 borophene planar Flow on TiO_2 (001) substrate after adsorption.

One of the key properties used to describe the photophysics and photochemistry of interfacial materials on substrates is the nature of the electrically excited states. For the χ3 borophene sheet on the TiO_2 (001) substrate, the interaction between the 2D metal sheet and the bulk TiO_2 (001) substrate gives rise to a rich χ3 borophene-to-TiO_2 (001) substrate charge transfer state. For the χ3 borophene sheet, the band dispersion shown in Fig. 3a reveals the perfect metallicity in both symmetry directions. The interfacing or adsorption of χ3 borophene sheet on the TiO_2 (001) substrate triggered the oxidation process and leached out the metallicity of the χ3 borophene sheet in all directions (Fig. 3b). Therefore, in this structure, the χ3 borophene atoms, which tend to donate electrons, bind more strongly to the TiO_2 (001) substrate surface and release more energy.

The interaction of oxygen atoms and their strong electronegativity in the TiO_2 (001) substrate with χ3 borophene sheet absorb charge density around the boron atoms (Figs. 4(a and b)), and the phase tends to exhibit semiconducting properties by introducing a small bandgap into the system.

Figure 5a shows that the adsorption of the χ3 borophene sheet on the TiO_2 (001) substrate reduces the anisotropy; the band crossings are lifted up and induce a narrow bandgap of ~0.238 – 0.369 eV. However, the presence of oxygen atoms and the formation of localized states were observed to reduce the electron mobility and electrical conductivity, whereas the presence of Ti should improve the mechanical properties.

To check the energetic stability of the χ3 borophene sheet on the substrate, we have calculated the binding energy using Eq. (2) to be 1.67 eV. Thus, the absorption is an exothermic process and is stable.

3.2 Density of state

The electronic structure was investigated to understand electron transfer and binding between each atom. Figs. 6(a) and 6(b, c and d) represent the total density of state (DOS) and partial density of state (PDOS) projected on each atomic species. The Fermi energy from the total density of state in Fig. 6 is 11.54state/eV; the total density of state shows a lot of structure that can be better understood by looking at PDOS. From 0 eV to 3 eV, the Ti-s, O-p, and B-p all contribute to the DOS, indicating a bond between them, which is the highest banding energy. For states ranging from -2 eV to -6 eV, only O-p, B-s, and B-p contribute to the total DOS. At -35 eV Ti-p is a significant contribution to the DOS along with B-p and O-s orbit, implying a bonding between them.

3.3 Electrostatic potential and work function

In order to understand the charge transfer mechanism at the

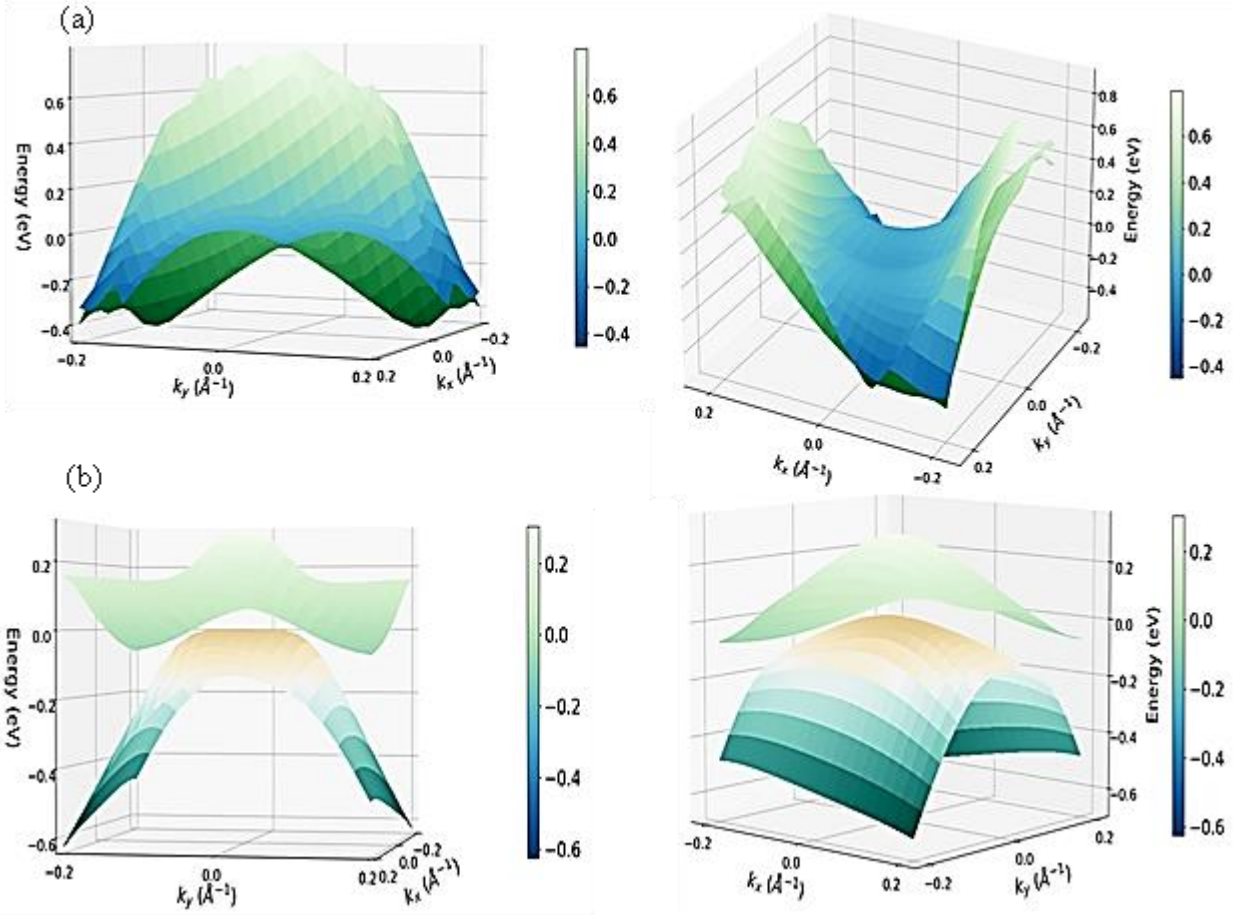

Fig. 3 (a) Band dispersion of conventional unit cell of the χ3-borophene monolayer in both symmetry directions (b) band dispersion of χ3-borophene monolayer interfaces with TiO2 (001) substrate in both symmetry directions.

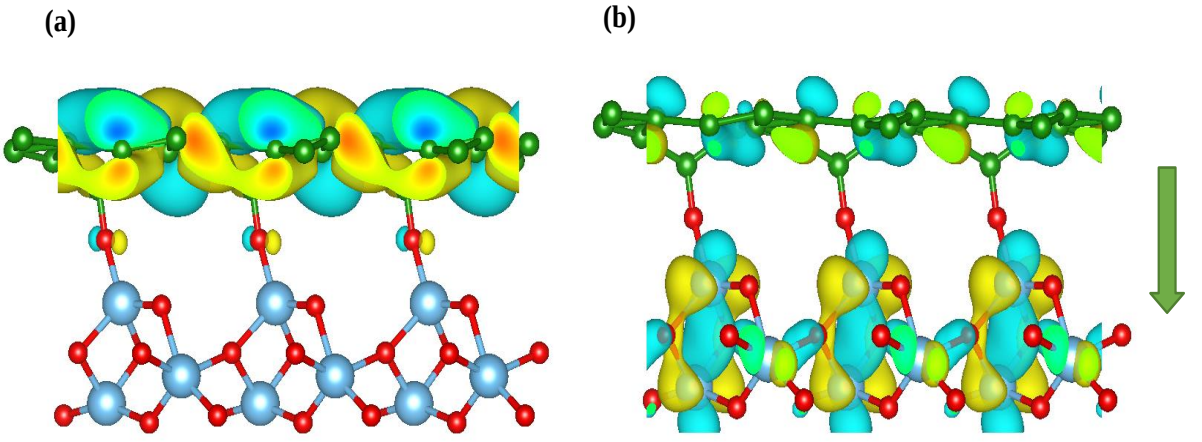

Fig. 4 (a) χ3-borophene monolayer charge absorption around the Boron atoms (b) TiO_2 (001) substrate charge density transfer.

interface of the χ3 borophene sheet on the TiO_2 (001) substrate, the electrostatic potential plot was analyzed. Moreover, the work function is a useful tool for studying the optical properties of 2D nanostructures. Understanding the effects of adsorption and the electrical properties of the system requires analysis of the averaged electrostatic potential plots of adsorbed molecules.

For instance, a gas sensor device composes of a receptor and a transducer. Immediately a gas molecule targets the receptor, and they induce a change in its properties such as mass, work function, dielectric constant, electrode potential, and so on.[22] Sosa *et al.*[21] show that the sensor work function depends on the chemical-physical surface processes.

The minimum energy required to move an electron from a solid surface to a place in the vacuum just outside the solid surface is called the work function of the material. The work function is strongly influenced by the surface on which the gas is adsorbed and affects the electrical conductivity of the material surface. The work function (Φ) can be determined by[21,23]

$$\Phi = E_{Vacuum} - E_{Fermi} \quad (3)$$

Where $\Phi$is the work function of the system, $E_{Vacuum}$is the Electrostatic Potential in the vacuum region, and $E_{Fermi}$is the Fermi energy. These values were obtained from first principle calculations.

Figures 7(a-c) show the Electrostatic Potential of the TiO_2 monolayer before absorption, the electrostatic potential of χ3 borophene sheet before absorption, and the electrostatic potential of χ3 borophene sheet absorbed on TiO_2 (001) substrate to be 2.11 eV, 2.59 eV, and 3.83 eV respectively. It can be observed from the plot that the electrostatic potential value of the borophene sheet interfaced on the TiO_2 substrate surfaces is higher than the TiO_2 monolayer and borophene sheet before adsorption. The differences in the potential of the interfaced sheet/monolayer from Borophene sheet before absorption; and interfaced sheet/monolayer from TiO_2 monolayer before adsorption are 1.24 eV and 1.72 eV, respectively. The net potential difference values are positive. This indicates a significant potential drop between the χ3 borophene sheet and TiO_2 (001) substrate interface, implying that there is a sufficient driving force for charge transfer from the borophene sheet to TiO_2. Also, there is adequate driving power for electron injection from χ3 borophene sheet to TiO_2.[24]

Comparing the estimated work function values to experimental data is not straightforward for various reasons. For starters might produce different findings. Firstly, different approaches for measuring the work function can sometimes lead to different results. It's worth noting that the work Function can be determined using both photoelectron spectroscopy and the Kelvin probe approach.[23,25] The first approach allows for absolute work function measurement, whereas the second simply provides a contact potential difference between the probe and the sample surface. However, utilizing a photoelectron spectroscopy calibration process, it is feasible to convert Kelvin probe findings into absolute values, allowing for a more consistent interpretation of the experimental data. Second, sample characteristics such as the existence of defects, doping and impurity concentration, and so on frequently impact experimental work function results. These factors influence experimental results but are difficult to include in ab-initio numerical models. Finally, the approximation inherent in the work function calculation method (in this case, the DFT-HSE06 approximation) is expected to give results very close to the experimental data.

Experimental results of work function on annealed and oxidized clean TiO_2 (001) surfaces reported by Shun *et al.*[26] range from 4.29 eV to 6.08 eV. The theoretically calculated work function value of TiO_2 (001) in this work was 5.13 eV which is within the experimental range. This validates the numerical approach used.

Table 1 shows the value of the work function of χ3 borophene, TiO_2 (001) monolayer, and χ3 borophene/ TiO_2 (001) interfaced. The work function value of χ3 borophene, TiO_2 (001) substrate and χ3 borophene/ TiO_2 (001) interfaced, given by Eq. 3, are 4.68 eV, 5.13 eV and 4.49 eV, respectively. This value changes significantly after the adsorption processes occur between the χ3 borophene sheet and TiO_2 (001)

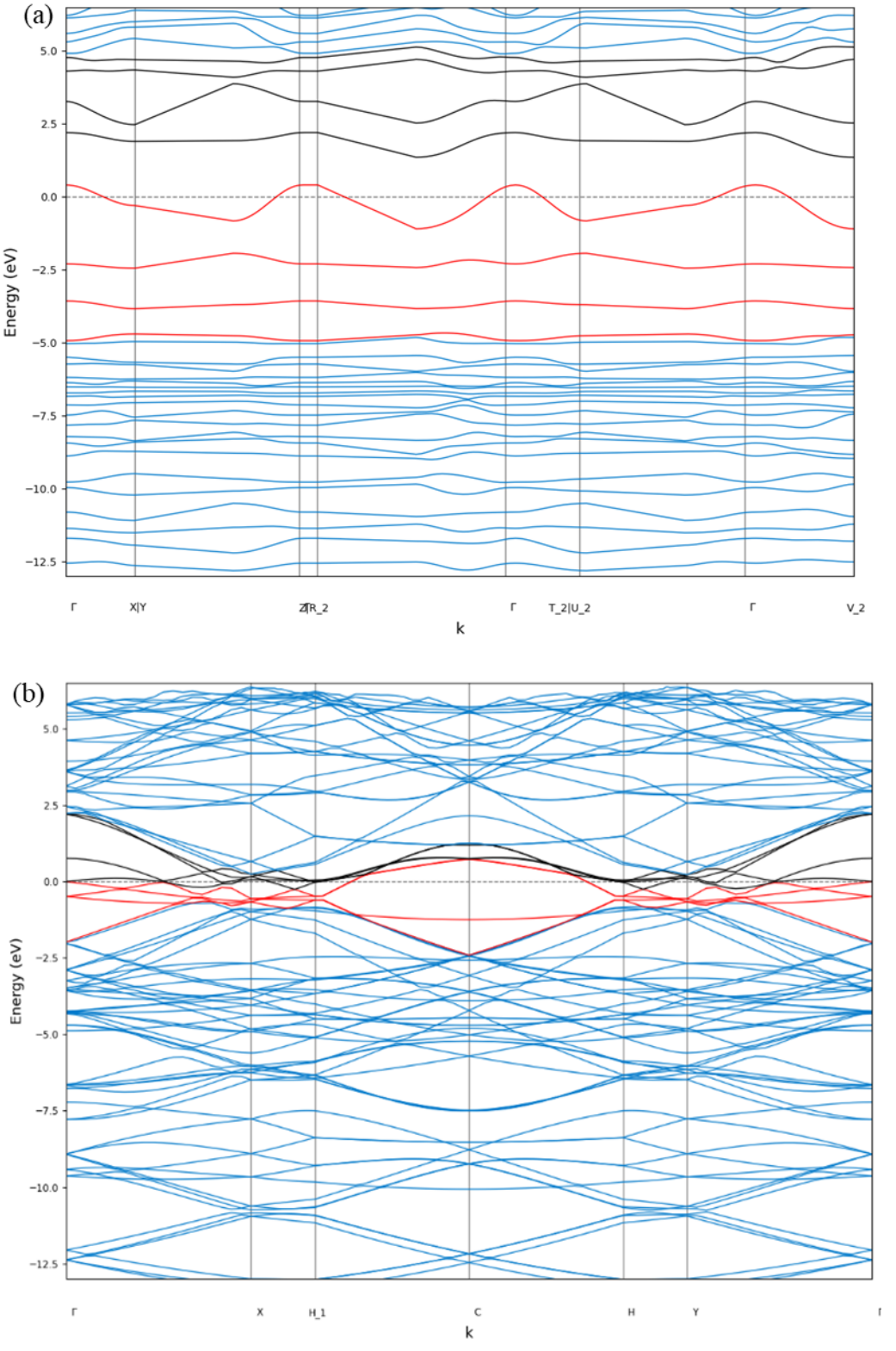

Fig. 5 (a) Band structure of the χ3 borophene sheet interfaced on the TiO_2 (001) substrate with a narrow band Gap (b) Band structure of the χ3 borophene sheet with no Band Gap.

monolayer. Interestingly, after the adsorption process, the corresponding work function of the interfaced materials is lower than the corresponding work function of both the χ3 borophene and the substrate. In summary, the work function for both materials in our study can be tuned through interfacing/adsorption processes, enabling their potential use as gas sensors and superconductors.

3.4 Optical properties

How light is reflected, absorbed, and transmitted depends on

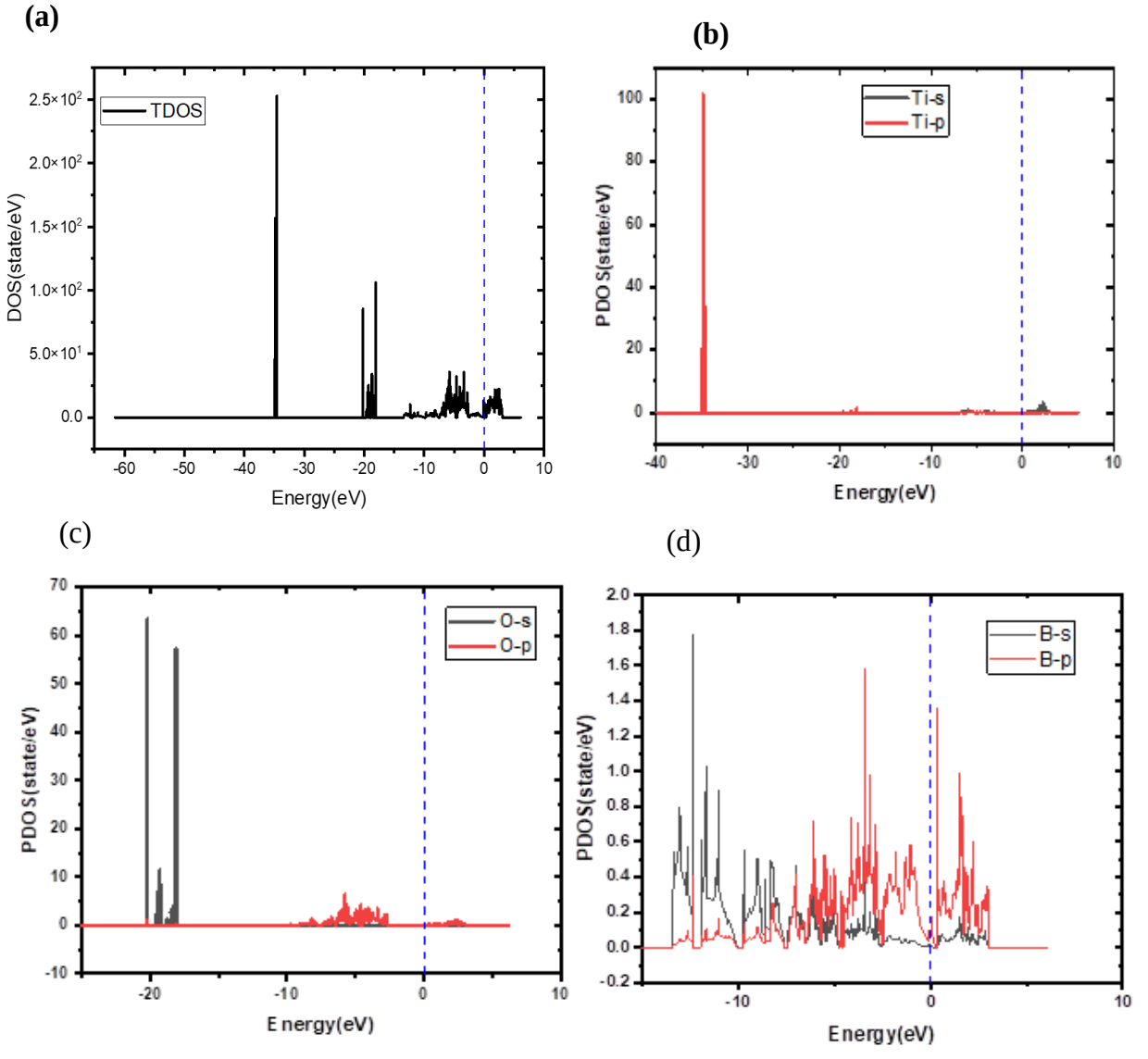

Fig. 6 (a) Total density of state of TiO_2B (The Fermi energy is set to 0eV) (b) Partial density of state of Ti in S-orbit and p-orbit (c) Partial density of state of O in s-orbit and p-orbit (d) Partial density of state for B in s-orbit and p-orbit.

Table 1. The calculated work function, fermi energy and electrostatic potential of χ3 borophene, TiO_2 (001) Monolayer and χ3 borophene /TiO_2 (001).

	Work function, Φ (eV)	Fermi energy (eV)	Electrostatic Potential (eV)	Ref.
χ3 borophene	4.68	-2.09096307	2.59	Present
TiO_2 (001) Monolayer	5.13	-3.02471217	2.11	Present
χ3 borophene /TiO_2 (001)	4.49	-0.66130352	3.83	Present

the optical properties of matter. Understanding a material's optical characteristics is essential for many applications, such as absorbers, optical coatings, reflectors, and other optoelectronic devices. In crystals, the dielectric function $\varepsilon(\omega)$ illustrates the connection between electric displacement and electric field in materials and shows how the medium interacts with incoming light of frequency. Understanding a solid's electrical structure is aided by studying its optical properties. The real and imaginary part $\varepsilon_1(\omega)$ and $\varepsilon_2(\omega)$ respectively, of complex dielectric function $\varepsilon(\omega)$, $\varepsilon(\omega) = \varepsilon_1(\omega) + i\varepsilon_2(\omega)$, is obtained from the momentum matrix elements between the occupied and the unoccupied electronic states. A direct approach is used to compute this[27,28]

$$\varepsilon_2(\omega) = \frac{2e^2\pi}{\Omega\varepsilon_0} \sum_{k,v,c} |\psi_k^c | u.r | \psi_k^v|^2 \delta(E_k^c - E_k^v - E) \quad (4)$$

where ψ_k^c *and* ψ_k^v are the conduction and valence band wave functions at k (wave number), ω is the light frequency, u is the vector defining the polarisation of the incident electric

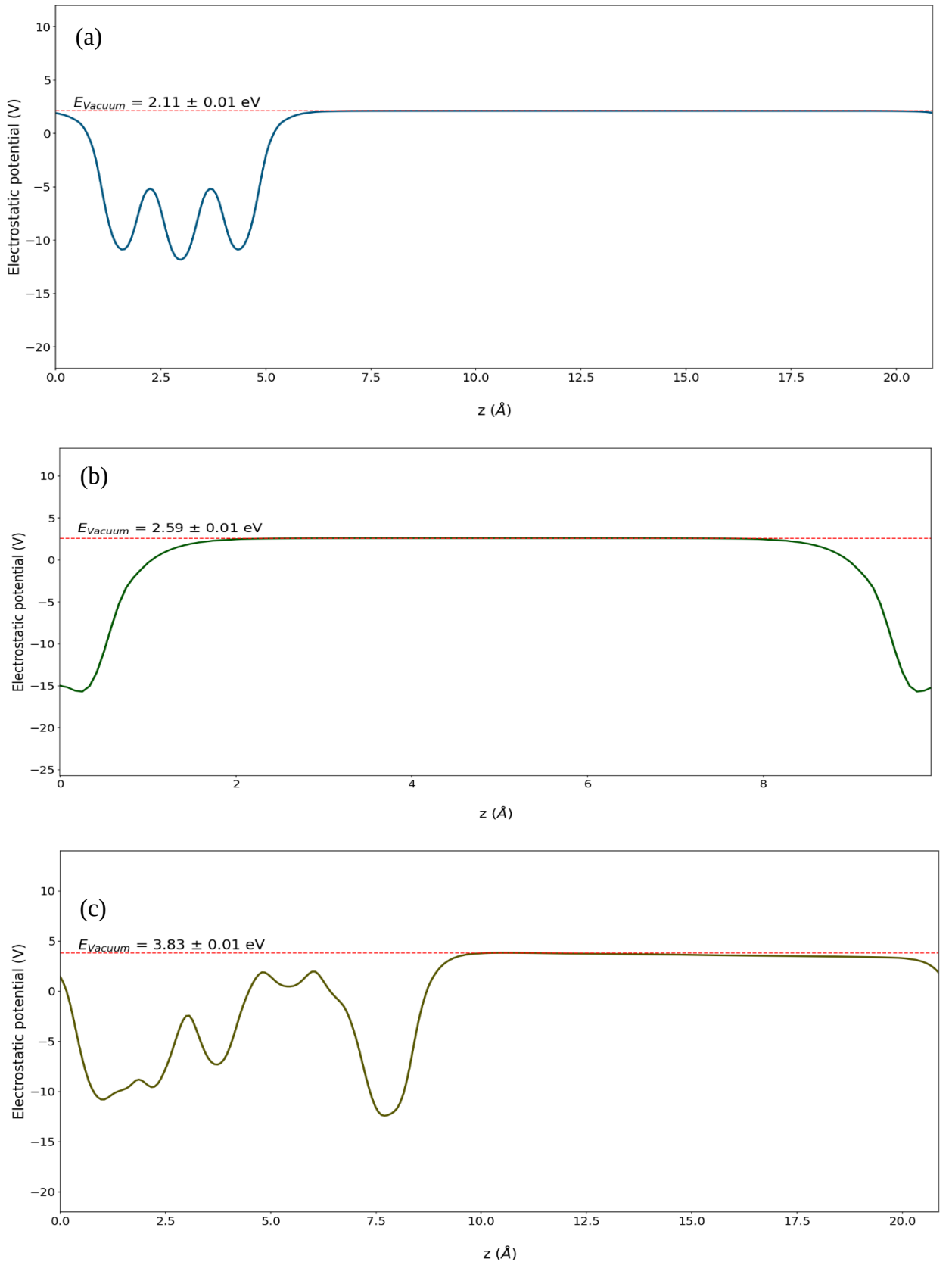

Fig. 7 (a) Electrostatic potential plot of TiO_2 (001) substrate (b) Electrostatic Potential Plot of χ3 borophene sheet. (c) Electrostatic Potential Plot of χ3 borophene sheet on TiO_2 (001) substrate.

field, and e is the electronic charge. The aforementioned property, along with a number of optical properties relating to photon energy, such as extinction coefficient $k(\omega)$, complex refractive index with real part $n(\omega)$, reflectance $R(\omega)$, real and imaginary optical conductivity $\sigma_1(\omega)$ and $\sigma_2(\omega)$, respectively, absorption coefficient $\alpha(\omega)$ and electron loss

function are used to measure the response to electromagnetic radiation. The electron excitation is linked to the peak value of the real component of the dielectric constant. The real component can be inferred from the imaginary part $\varepsilon_2(\omega)$ via the Kramers-Kronig connection.[27,29]

Semiconductors and insulators, in contrast to metals, contain bonded valence electrons. This characteristic leads to interband transitions. When the semiconductor electrode is illuminated, excited electrons are created in the conduction band, and holes are created in the valence band. Some recombine via radiation to produce a luminescence emission known as photoluminescence (PL). Radiative recombination can occur directly between the conduction and valence bands (interband transitions) or at specific impurity or defect levels within the bandgap where trapped electrons, holes, or both exist.[30] Interband transitions, which are classified into direct and indirect transitions based on the transition mode, are the primary source of light emission (luminescence). This transition is direct when the electron jumps between VBM (valence band maximum) and CBM (conduction band minimum) at the same point. In contrast, indirect transitions occur. This prerequisite makes it evident that metals with free electrons have the highest optical effects and are thus the ideal materials for researching the electrical characteristics of resonant particle phonons. These metals have filled valence bands but only partially filled conduction bands. Although most metals display distinct inter-band transitions, the ideal free electron metals response is based on the conduction electrons.[31] When there is just one free electron in a metallic system, that electron is not entirely free to travel, and the optical transitions of that electron at deeper levels (like the nucleus) significantly impact the dielectric response. These interband excitations dramatically alter the dielectric function. Interband shifts, which are excluded from the Drude model[32,33], however, contribute to the imaginary component of $\sigma_2(\omega)$, at high frequencies in actual metals, resulting in absorption losses.[34,35]

At room temperature, we estimate the optical properties of χ3 borophene sheet/TiO_2 substrate. It is understandable from Fig. 8 that χ3 borophene sheet/TiO_2 substrate is optically anisotropic. When radiation is polarized in the z-plane, where the x, y, and z directions are aligned in the a, b, and c axes of the lattice system, it reflects differently than polarized radiation in the corresponding x or y plane.

For photon energies up to 25 eV, the predicted optical functions of χ3 borophene sheet/TiO_2 substrate are shown in Fig. 8. Fig. 8(a) depicts the real and imaginary components of the complex dielectric constant (Permittivity)) of the χ3 borophene sheet on the TiO_2 (001) substrate as a function of the photons. When an electric field is applied, the magnitude $\varepsilon_1(\omega)$ indicates how much the material is polarised by the creation of electric dipoles within the material, whereas the quantity $\varepsilon_2(\omega)$ denotes absorption within the substance. When $\varepsilon_2(\omega) = 0$, it denotes transparency; when absorption occurs, $\varepsilon_2(\omega) \neq 0$. For the real part $\varepsilon_1(\omega)$ of the dielectric function, the highest peak for χ3 borophene sheet/TiO_2 substrate that appears within the visible light range appears around 2.07eV. In contrast, the imaginary part $\varepsilon_2(\omega)$ indicate that its maximum peak occurs in the visible light range at about 2.23eV, which is related to this study's estimated band gap. When the value $\varepsilon_2(\omega)$ at about 12eV hits zero, it was seen that the interfaced material becomes transparent. The static dielectric constant of χ3 borophene sheet on the TiO (001) substrate is 5.61 (~6), suggesting that this material may be a suitable dielectric material. Furthermore, the bonded materials were shown to exhibit semiconducting properties in the energy region of $\varepsilon_1(\omega) > 0$.

Absorption coefficients provide information about the maximum efficiency of solar energy conversion, indicating the distance that light of a particular wavelength can travel through the material before being absorbed. The approximate bandgap of the material, 0.22 eV, is where the absorption begins (Fig. 8(c)). The spectra's ultraviolet region observed firm absorption peaks of 5.10eV, 7.24ev, and 7.69ev, respectively. The presence of absorption peaks in the visible region confirms the partial transparency of the material.

Although their peak values differ, the optical conductivity and absorption coefficient have comparable numbers. The photoelectronic characteristics of the material, whose electrical conductivity is as a result of the interband transitions along the x-axis and rises as a result of electromagnetic radiation absorption, are depicted in Fig. 8(b). The predicted bandgap of the study corresponds to the first peak detected at approximately 0.22 eV. The fact that the material has a very small bandgap, as seen from the band structure, can also be used to confirm that photoconduction starts at nearly zero photon energy. Additionally, it was shown in this study that when the photon energy is higher than 12eV, there is no optical conductivity.

The percentage reflectance as a function of photon energy is shown in Fig. 8(e). The materials` reflectivity is shown to increase in the infrared region, with an approximate percentage value of 40 in the y- plane, before declining. One could see that the χ3 borophene sheet/TiO_2 substrate had a high reflectivity in the Infrared Region (IR)- Visible Region-Ultraviolet Region (UV). This material did not exhibit reflectance above a photon energy of 12eV photon energy.

The energy-dependent loss function and refractive index are displayed in Figs. 8(d) and (f). At photon energy of 21.66 eV, the maximum energy loss function (ω_p) for fast electrons passing through the material was recorded. This Bulk Plasma frequency ω_p at its peak value occurs when $\varepsilon_1(\omega) = 0$ and $\varepsilon_2(\omega) < 0$. The material become transparent when the incident photon frequency exceeds ω_p. The complex refractive index in eV's is shown as an energy function in Fig. 8(f). In this study, the Infrared Region has the highest static refractive index $n(0)$, measuring 2.59 in the x-plane. A measure of the phase velocity of an electromagnetic wave in a medium and the attenuation of an electromagnetic wave as it passes through the material are described by the real and

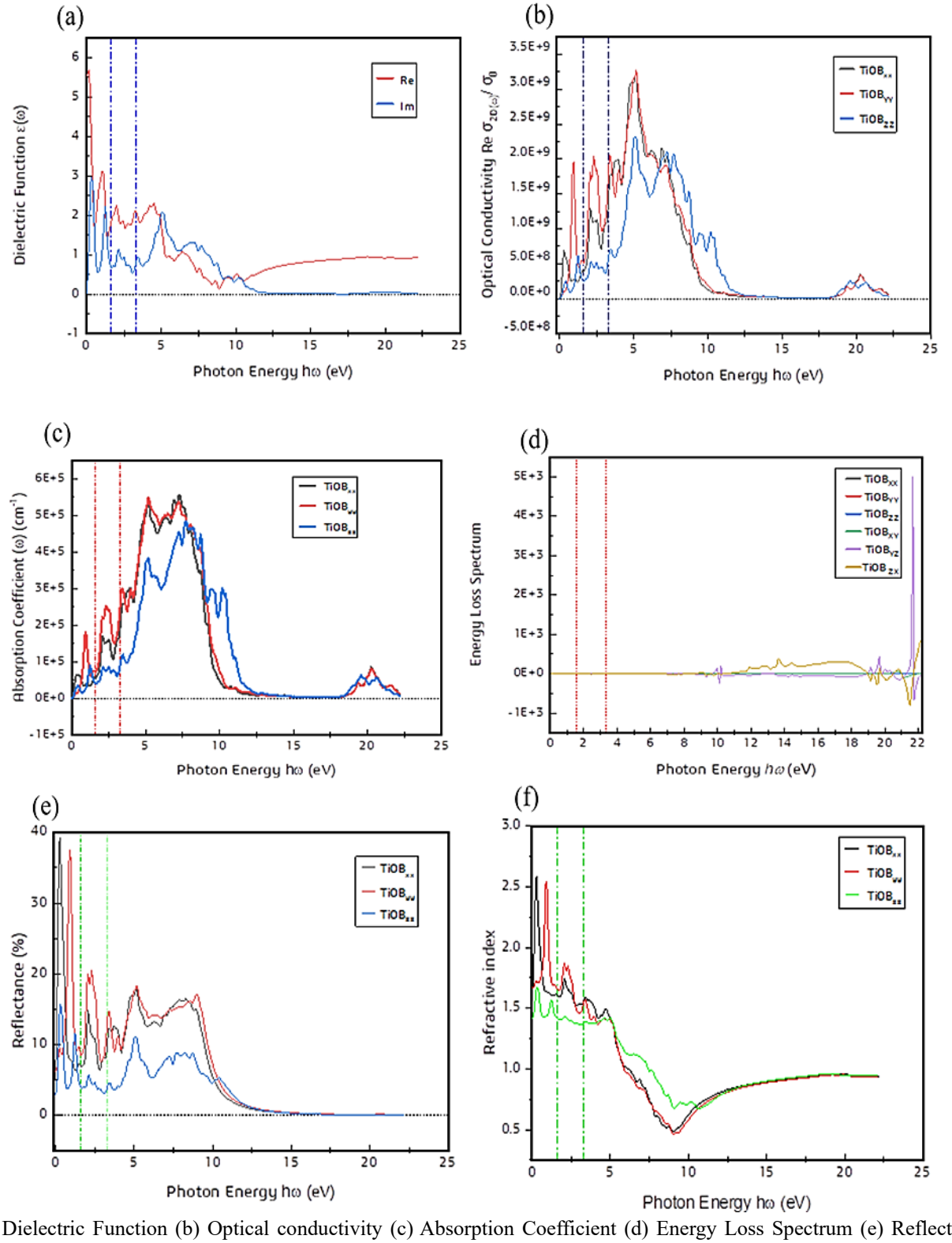

Fig. 8 (a) Dielectric Function (b) Optical conductivity (c) Absorption Coefficient (d) Energy Loss Spectrum (e) Reflectance (f) Refractive Index.

imaginary components of the refractive index, respectively.

4. Conclusion

Herein, the first principle approach was adopted to evaluate the structural, electronic, and optical properties of χ3 borophene sheet/TiO_2 substrate using VASP simulation package. Also, the effect of substrate on the stability of borophene was studied. The structure of the χ3 borophene sheet/TiO_2 substrate changes upon contact with a binding energy of 1.67 eV, and the structure of the interfacial system is stable. These systems are capable of absorbing visible light as they have the earliest absorption peaks at visible and

ultraviolet frequencies. This supports partial transparency in materials. Significant photoconductivity was observed in the photon energy range below 12 eV. Our results show that the optoelectronic properties of the χ3 borophene sheet/TiO_2 substrate are tunable, which may be useful for various applications. The interplanar distances and work function are equal to 1.38 Å, and 4.49eV, respectively. We concluded that the low interplanar distances and high adhesion energies indicate good interfacial interaction and stable bonding. However, the high work function determined by the study indicates suitable sensor property of the new material. The material exhibits good optical properties, thus becoming a good option for superconductors, coating, and sensors. It is possible to conclude that the study will play an essential role in developing current technologies based on the projected qualities.

Acknowledgement
The authors would like to thank the financial support from the University of Johannesburg Research Committee (URC), the National Research Foundation, and Jen would like to acknowledge the financial support from the National Research Foundation of South Africa. Computational simulations and calculations were partially performed using computational resources of the CSIR`s Centre for High-Performance Computing in South Africa.

Conflict of Interest
The authors declare no conflict of interest.

Supporting Information
Not applicable.

References
[1] F. Zergani, Z. Tavangar, A thorough study on the F-decoration of χ3 borophene and enhancement of anodic performance of Lithium-ion batteries, *Journal of Molecular Liquids*, 2020, **319**, 114343, doi: 10.1016/j.molliq.2020.114343.
[2] E. S. Penev, A. Kutana, B. I. Yakobson, Can two-dimensional boron superconduct? *Nano Letters*, 2016, **16**, 2522-2526, doi: 10.1021/acs.nanolett.6b00070.
[3] Z.-Q. Wang, T.-Y. Lü, H.-Q. Wang, Y. P. Feng, J.-C. Zheng, Review of borophene and its potential applications, *Frontiers of Physics*, 2019, **14**, 1-20, doi: 10.1007/s11467-019-0884-5.
[4] A. A. Kistanov, Y. Cai, K. Zhou, N. Srikanth, S. V. Dmitriev, Y.-W. Zhang, Exploring the charge localization and band gap opening of borophene: a first-principles study, *Nanoscale*, 2018, **10**, 1403-1410, doi: 10.1039/c7nr06537j.
[5] G. Bhattacharyya, A. Mahata, I. Choudhuri, B. Pathak, *Journal of Physics D: Applied Physics*, 2017, **50**, 405103, doi: 10.1088/1361-6463/aa81b8.
[6] Y. Liu, E. S. Penev, B. I. Yakobson, Probing the synthesis of two-dimensional boron by first-principles computations, *Angewandte Chemie International Edition*, 2013, **52**, 3156-3159, doi: 10.1002/anie.201207972.
[7] X. Sun, X. Liu, J. Yin, J. Yu, Y. Li, Y. Hang, X. Zhou, M. Yu, J. Li, G. Tai, W. Guo, Two-dimensional boron crystals: structural stability, tunable properties, fabrications and applications, *Advanced Functional Materials*, 2017, **27**, 1603300, doi: 10.1002/adfm.201603300.
[8] B. Feng, J. Zhang, Q. Zhong, W. Li, S. Li, H. Li, P. Cheng, S. Meng, L. Chen, K. Wu, Experimental realization of two-dimensional boron sheets, *Nature Chemistry*, 2016, **8**, 563-568, doi: 10.1038/nchem.2491.
[9] K. Fradi, A. Bouich, B. Slimi, R. Chtourou, towards improving the optoelectronics properties of $MAPbI_{3(1-x)}B_3x$/ZnO heterojunction by bromine doping, *Optik*, 2022, **249**, 168283, doi: 10.1016/j.ijleo.2021.168283.
[10] Z. Xia, X. Chen, W. Zhang, J. Li, B. Xiao, H. Du, Enhancement of lithium-ion hopping on halogen-doped χ3 borophene, *Physical Chemistry Chemical Physics*, 2018, **20**, 24427-24433, doi: 10.1039/c8cp03803a.
[11] P. Blöchl, Projector augmented-wave method, *Physical Review B*, 1994, **50**, 17953–17979, doi: 10.1103/PhysRevB.50.17953.
[12] G. Kresse, J. Furthmüller, J. Hafner, Ab initio force constant approach to phonon dispersion relations of diamond and graphite, *Europhysics Letters* (EPL), 1995, **32**, 729-734, doi: 10.1209/0295-5075/32/9/005.
[13] G. Kresse, Ab initio molecular dynamics for liquid metals, *Journal of Non-Crystalline Solids*, 1995, **192-193**, 222-229, doi: 10.1016/0022-3093(95)00355-x.
[14] G. Kresse, J. Furthmüller, Efficiency of ab-initio total energy calculations for metals and semiconductors using a plane-wave basis set, *Computational Materials Science*, 1996, **6**, 15-50, doi: 10.1016/0927-0256(96)00008-0.
[15] A. Togo, I. Tanaka, First principles phonon calculations in materials science, *Scripta Materialia*, 2015, **108**, 1-5, doi: 10.1016/j.scriptamat.2015.07.021.
[16] J. Heyd, G. E. Scuseria, M. Ernzerhof, Hybrid functionals based on a screened Coulomb potential, *The Journal of Chemical Physics*, 2003, **118**, 8207-8215, doi: 10.1063/1.1564060.
[17] Z. Zhang, Y. Yang, G. Gao, B. I. Yakobson, Two-dimensional boron monolayers mediated by metal substrates, *Angewandte Chemie*, 2015, **127**, 13214-13218, doi: 10.1002/ange.201505425.
[18] M. Fazilaty, M. Pourahmadi, M. R. Shayesteh, S. Hashemian, Investigating and comparing structural, electronic and optical properties of χ3-Borophene in monolayer, nanoribbon and nanotube modes as a transparent metal, *Journal of Physics and Chemistry of Solids*, 2021, **148**, 109683, doi: 10.1016/j.jpcs.2020.109683.
[19] C. Zhang, Z. Zhang, W. Yan, X. Qin, Effect of doping on the photoelectric properties of borophene, *Advances in Condensed Matter Physics*, 2021, **2021**, 1-7, doi: 10.1155/2021/3718040.
[20] F. B. van Duijneveldt, J. G. C. M. van Duijneveldt-van de Rijdt, J. H. van Lenthe, State of the art in counterpoise theory, *Chemical Reviews*, 1994, **94**, 1873-1885, doi: 10.1021/cr00031a007.
[21] A. N. Sosa, J. E. Santana, Á. Miranda, L. A. Pérez, R. Rurali,

M. Cruz-Irisson, Transition metal-decorated germanene for NO, N_2 and O_2 sensing: a DFT study, *Surfaces and Interfaces*, 2022, **30**, 101886, doi: 10.1016/j.surfin.2022.101886.
[22] N. Yamazoe, K. Shimanoe, Chapter One - Fundamentals of semiconductor gas sensors, Editor(s): Raivo Jaaniso, Ooi Kiang Tan, In Woodhead Publishing Series in Electronic and Optical Materials, Semiconductor Gas Sensors (Second Edition), Woodhead Publishing, 2020, 3-38, doi: 10.1016/B978-0-08-102559-8.00001-X.
[23] M. Bertocchi, M. Amato, I. Marri, S. Ossicini, Tuning the Work Function of Si(100) Surface by Halogen Absorption: A DFT Study, *Physica Status Solidi C Current Topics in Solid State Physics*, 2017, **14**, 1–6, doi: 10.1002/pssc.201700193.
[24] N. K. Pham, N. H. Vu, V. van Pham, H. K. T. Ta, T. M. Cao, N. Thoai, V. C. Tran, Comprehensive resistive switching behavior of hybrid polyvinyl alcohol and TiO_2 nanotube nanocomposites identified by combining experimental and density functional theory studies, *Journal of Materials Chemistry C*, 2018, **6**, 1971-1979, doi: 10.1039/c7tc05140a.
[25] I. Borriello, G. Cantele, D. Ninno, G. Iadonisi, M. Cossi, V. Barone, Ab initio study of electron affinity variation induced by organic molecule adsorption on the silicon (001) surface, *Physical Review B*, 2007, **76**, 035430, doi: 10.1103/physrevb.76.035430.
[26] S. Kashiwaya, J. Morasch, V. Streibel, T. Toupance, W. Jaegermann, A. Klein, The work function of TiO_2, *Surfaces*, 2018, **1**, 73-89, doi: 10.3390/surfaces1010007.
[27] M. Roknuzzaman, A. K. M. A. Islam, Ab initio investigation of nitride in comparison with carbide phase of superconducting InX (X = C, N), *ISRN Condensed Matter Physics*, 2013, **2013**, 1-9, doi: 10.1155/2013/646042.
[28] M. Othman, E. Kasap, N. Korozlu, The structural, electronic and optical properties of InxGa1−xP alloys, *Physica B: Condensed Matter*, 2010, **405**, 2357-2361, doi: 10.1016/j.physb.2010.02.051.
[29] M. M. Hossain, First-principles study on the structural, elastic, electronic and optical properties of $LiNbO_3$, *Heliyon*, 2019, **5**, e01436, doi: 10.1016/j.heliyon.2019.e01436.
[30] E. McCann, M. Koshino, The electronic properties of bilayer graphene, *Reports on Progress in Physics*, 2013, **76**, 056503, doi: 10.1088/0034-4885/76/5/056503.
[31] D. P. Rai, C. E. Ekuma, Origin of strong Coulomb interactions in borophene: first-principles Wannier function analysis, *Journal of Applied Physics*, 2022, **131**, 145105, doi: 10.1063/5.0088860.
[32] L. A. Falkovsky, A. A. Varlamov, Space-time dispersion of graphene conductivity, *The European Physical Journal B*, 2007, **56**, 281-284, doi: 10.1140/epjb/e2007-00142-3.
[33] L. A. Falkovsky, S. S. Pershoguba, *Physical Review B-Condensed Matter Materials Physics*, 2007, **76**, 153410, doi: 10.1103/PhysRevB.76.153410.
[34] C. C. Homes, S. Khim, A. P. MacKenzie, Perfect separation of intraband and interband excitations in $PdCoO_2$, *Physical Review B*, 2019, **99**, 195127, doi: 10.1103/physrevb.99.195127.
[35] C. Ambrosch-Draxl, J. O. Sofo, Linear optical properties of solids within the full-potential linearized augmented planewave method, *Computer Physics Communications*, 2006, **175**, 1-14, doi: 10.1016/j.cpc.2006.03.005.

Author Information

Ayotunde Idris Ibitoye *is currently a Masters Research student in Mechanical Engineering Science at the University of Johannesburg (UJ). Being a member of the JENANO Research Group at the University of Johannesburg, his research interest focuses on Nanotechnology, Organic Solar Cells, Semiconductors, Dielectrics, Piezoelectric, Smart materials, and associated processes (e.g., Atomic layer deposition (ALD), Spark Plasma Sintering (SPS)). He has garnered expertise in Quantum computing (Atomic Simulation environment and Python), Density functional Theory (DFT), Ab-Initio MD (Ab-Initio Molecular Dynamics using VASP), Molecular Dynamics (Soft Matters MD using GROMAC code) in predicting Semiconducting properties, Photoelectric Properties, Adsorption, Absorption, Diffusivity, Permeability, Activation energy, Electronics and Optical Properties. Skilled in Thin-Film depositions using Vapour deposition processes, Nanoparticles synthesis, Dye synthesis, Material characterizations, DOS, Data analytics, Catalysis and Embrittlement studies. He was recently a Guest Speaker at Green Hydrogen Economy – "Hit or Hindrance" organized by Climate Innovation Centre, South Africa. He also represented his Research Group in Gauteng Accelerator Programme (GAP) GREEN and got a Special Recognition Award. He has a B. Eng. (Hons) in Metallurgical and Materials Engineering. He has accumulated rich experience in Furnace Repair and Maintenance, Computer Networking, and Solar Power installation with Maintenance. In nanotechnology and material science fields, he has research articles published in international journals and conferences.*

Oriyomi Rasak Opetubo*, is currently a Master's student at the department of Mechanical Engineering at the University of Johannesburg, South Africa. He holds his Bachelor of Science degree in Mechanical Engineering at Olabisi Onabanjo University, Nigeria. He is a member of the Nigerian Society of Engineers (NSE) and the Nigerian Institute of Management (NIM). He is an experienced power plant Engineer and a researcher He is also a member of the JENANO Research Group with a research focus on Hydrogen generation, purification and storage using density functional theory (DFT) and Molecular dynamic*

(MD), water desalination, carbon capture and storage (CCS), thin film solar cell, biomass, Energy optimization and manufacturing of nanomaterial using Atomic Layer Deposition (ALD).

Dr Sunday Temitope Oyinbo *received his PhD in Mechanical Engineering Science from the University of Johannesburg (UJ). He is currently a postdoctoral research fellow at the University of Johannesburg. As a member of the JENANO Research Group at the University of Johannesburg, his research interest focuses on nanotechnologies and associated processes (e.g. Atomic layer deposition (ALD) and cold gas dynamic spray (CGDS)). He has accumulated rich research experience in the microstructure reconstruction of metal matrix composite and hydrogen purification technology. He has research expertise in computational modelling and simulation, materials and microstructural characterization, finite element analysis (FEA), molecular dynamics (MD), density functional theory (DFT), and proficient knowledge in programming (LAMMPS code, Python script, VASP code). At present, the ultra-thin film composite metal membrane experiment platform has been built through computational modelling and surface functionality in the absorption and separation of gas through the nanoporous membrane has been achieved. He has published various research papers in International Journals and Conferences in the areas of nanotechnology and material science.*

Prof Jen *received his PhD from the University of California, Los Angeles. In August 2015, Prof. Jen joined the Mechanical Engineering Science Department as a Full Professor at the University of Johannesburg. Currently, Prof. Jen also serves as the Head of Department of the Mechanical Engineering Science. Prof Jen has very significant research outputs and performances. So far, Prof Jen has various research papers in International Journals, books and Conferences. Prof Jen has chaired two international conferences and delivered numerous Keynote speeches in international conferences. He has been recognized as one of the top researchers in the field of Mechanical Engineering; this is evident through his position as an ASME (American Society of Mechanical Engineers) Fellow. He is a highly regarded and well-respected professor and researcher. Very recently, due to his significant scientific contributions, he has been recognized and inducted by the Academy of Science of South Africa as a Fellow. He has made numerous and extensive contributions to the field of Mechanical Engineering, specifically in the areas of advance manufacturing processes and Renewable Energy.*

David Sibanda *received his B. Eng. (Hons) from the National University of Science and Technology, Bulawayo Zimbabwe in 2016. He joined the University of Johannesburg in 2021 for a Master of Engineering in Mechanical Engineering program. He has research interests in atomic layer deposition (ALD), superconductors, molecular dynamics, density functional theory and machine learning. He has published two papers in atomic layer deposition and density functional theory.*

Oluwatoyin Ewuola *has a Bachelor's degree in Agricultural Engineering from Obafemi Awolowo University, Ile-Ife, Nigeria and a MPhil degree in Mechanical Engineering from the University of Johannesburg, South Africa. He is currently studying towards a Doctoral degree in Mechanical Engineering from the University of Johannesburg. He is a member of the organising committee of the International Conference on Sustainable Materials Processing and Manufacturing conference series. He is also a member of the JENANO research group of the University of Johannesburg. He is currently a faculty in the department of Physics, University of Johannesburg. His research interests are Cold Gas Dynamics Spray deposition, Hydrogen generation/filtration, friction stir welding, Composite Metal Membranes, numerical simulations, renewable energy and material processing and characterization.*

